Novel Phthalocyaninatobis(alkylcarboxylato)silicon(IV) Compounds: NMR Data and X-ray Structures To Study the Spacing Provided by Long Hydrocarbon Tails That Enhance Their Solubility

Jose L. Sosa-Sánchez,*[a] Arturo Sosa-Sánchez,[a] Norberto Farfán,[b] Luis S. Zamudio-Rivera,[c] Gerson López-Mendoza,[c] Javier Pérez Flores,[d] and Hiram I. Beltrán*[c]

Abstract: The reaction between *trans*-$PcSiCl_2$ (**1**) and the potassium salts of six fatty acids (**2a–2f**) led to the *trans*-$PcSi[OOC(CH_2)_nCH_3]_2$ compounds (**3a–3f**), which were characterised by elemental analysis, IR, UV/Vis and ^1H, ^{13}C, and ^{29}Si NMR spectroscopy. From a detailed study of the NMR spectra, the strong anisotropic currents of the Pc macrocycle were found to have an effect on up to the sixth methylenic group. As expected, the length of the hydrocarbon tail does not affect the chemical shift of the ^{29}Si nucleus of any of the compounds, appearing at around −222.6. The structures of PcSi-$[OOC(CH_2)_nCH_3]_2$, where $n=7$, 10, 12, 13 and 20, were determined by X-ray crystallography. All the compounds were found to be triclinic with a $P\bar{1}$ space group. In all cases the observed crystallographic pseudosymmetry is C_i and the asymmetric unit consists of half a molecule. The silicon atom is at the centre of a distorted octahedron and hence its coordination number is six. The carboxylate fragments are in a *trans* configuration with respect to the Pc macrocycle. The supramolecular structures are discussed in detail herein. The correlation between the ^1H NMR chemical shifts and the position of the corresponding carbon atoms in the hydrocarbon tail reveals that the dicarboxylate substituents exhibit a spacer-like behaviour that enhances the solubility. A detailed study of the tail variable allowed us to evaluate the loss of radial shielding along the Pc^{2-} ligand.

Keywords: NMR spectroscopy · phthalocyanines · silicon · spacer groups · supramolecular chemistry

Introduction

The applications of (metallo)phthalocyanines (MPcs or Pcs) have been considerably extended since their discovery.[1–11] Owing to the strong intermolecular π–π stacking observed in planar MPcs and their inherent lack of solubility, single-crystal X-ray studies of these compounds are scarce[12–14] and their molecular characterisation by solution analysis is not possible; this has prevented, to some extent, the development of their chemistry and their widespread application. Only a few of their NMR spectra have been published in the literature[11] and detailed mass spectrometric analyses of these complexes are rarely found in recently published papers.[11] In addition, few studies on the solution electrochemistry of this family of compounds have been published even though they exhibit rich redox activity.[11]

In an effort to circumvent the problem of poor solubility, molecular engineering has provided some useful strategies with which to obtain soluble Pcs. As a result, more materials

[a] Dr. J. L. Sosa-Sánchez, A. Sosa-Sánchez
Centro de Investigación en Dispositivos Semiconductores
Instituto de Ciencias, BUAP, Blvd. 14 Sur y Av. San Claudio
Ciudad Universitaria Puebla, Puebla (Mexico)
E-mail: jose.sosa@icbuap.buap.mx

[b] Dr. N. Farfán
Departamento de Química, CINVESTAV
Apartado Postal 14–740, C. P. 07000 Mexico, D. F. (México)

[c] Dr. L. S. Zamudio-Rivera, G. López-Mendoza, Dr. H. I. Beltrán
Programa de Ingeniería Molecular, IMP
Eje Central Lázaro Cárdenas 152
Col. San Bartolo Atepehuacan, C. P. 07730, D. F. (Mexico)
Fax: (+52) 55-9175-6239
E-mail: hbeltran@imp.mx

[d] Dr. J. Pérez Flores
Instituto de Química-UNAM, Circuito Exterior, Ciudad Universitaria
Coyoacán, C. P. 04510, D. F. (Mexico)

 DOI: 10.1002/chem.200500003

have been produced for use in different applications.[15–17] Insoluble Pcs can be converted into soluble ones mainly by inner (nonperipheral)/outer (peripheral)/axial substitution with phase transfer/spacing groups attached to at least one of these three positions (Figure 1). When covalent axial substitution was used as the design variable, an oxidation state at the metallic centre of between +3 and +5 was needed.[11,12,15–18] Very recently, another approach was used to modify the planarity of the Pc macrocycle with a concomitant increase in solubility; the key design variable in this case was the placement of bulky groups at the inner (nonperipheral) positions of the Pc ligand[19] (Figure 1).

Since the MPcs derived from Group 14 elements (mainly from silicon and tin) have recently been found to have different applications,[11] much effort has been made to obtain a wide variety of such compounds.[11] However, most of the materials obtained are of a low solubility; consequently X-ray structures of Group 14 MPcs are rarely found in the literature.[12–14]

At present, our research group is working on silicon/germanium/tin MPc chemistry.[18,20] To prepare soluble MPcs, we have only considered the axial substitution of MPcs in our recent research;[18,20] we have also performed experiments that show the designed SnPcs have potential as corrosion inhibitor prototypes.[20]

Notwithstanding the problems involved in the analysis of SiPcs, one goal of this work was to completely characterise a family of axial dicarboxylate-substituted SiPcs through solution spectroscopic measurements as well as by single-crystal X-ray structure elucidation and to gain an insight into the main effects on these compounds of axial substitution with simple, linear carboxylate moieties. Another aim of this study was to determine the necessary length of the axial hydrocarbon tail required to achieve enough spacing to avoid π···π stacking forces and to increase the solubility of these SiPcs.

Results and Discussion

Herein we describe a simple methodology that involves the replacement of the chlorine atoms of the $SiPcCl_2$ (**1**) precursor with the respective carboxylic moiety of the fatty acid as its potassium salt (**2a–2f**) to obtain *trans*-PcSi-$[OOC(CH_2)_nCH_3]_2$ compounds (**3a–3f**) (Scheme 1). The transformations were carried out by microwave irradiation of the starting materials in *N*,*N*-dimethylformamide for 10 min at 600 W. The title compounds were characterised through elemental analyses, ^{1}H, ^{13}C and ^{29}Si NMR, IR and UV/VIS spectroscopy and single-crystal X-ray diffraction. The numbering system used in the NMR data of compounds **3a–3f** is shown in Scheme 1.

NMR trends: ^{1}H, ^{13}C and ^{29}Si NMR data were obtained for all the compounds studied (see Experimental Section). These systems possess inversion centres, and thus the observed signals correspond to a quarter of the Pc ring system owing to a local D_{4h} symmetry and to half of the hydrocarbon tails owing to C_i symmetry, in accord with the integrated ^{1}H NMR spectra. The two aromatic ^{1}H NMR signals for the hydrogen atoms in the Pc system behave as a second-order system owing to the magnetic nonequivalency of the nuclei. The chemical shifts for the ^{1}H signals of the hydrocarbon tail have a large spread owing to anisotropic effects in the methylenic -$(CH_2)_n$- protons (n=1–6) located inside the shielding cone of the Pc macrocycle. The most shielded signal is, in all cases, (standard deviation is given in parentheses) H-11 at $\delta=-0.92(4)$ ppm, followed by H-12 at $\delta=-0.71(3)$ ppm and H-10 at $\delta=-0.60(4)$ ppm. For H-13, H-14 and H-15, the shielding effect is moderate, relative to the three former signals, appearing at $\delta=0.10(3)$, 0.56(2) and 0.84(2) ppm, respectively. The remaining signals are more difficult to assign as a result of signal overlapping.

The ^{13}C NMR signals for the carbon atoms in the Pc system were assigned as follows (standard deviation in parenthesis): C-1,8 at $\delta=150.1(5)$ ppm, C-2,7 at $\delta=$

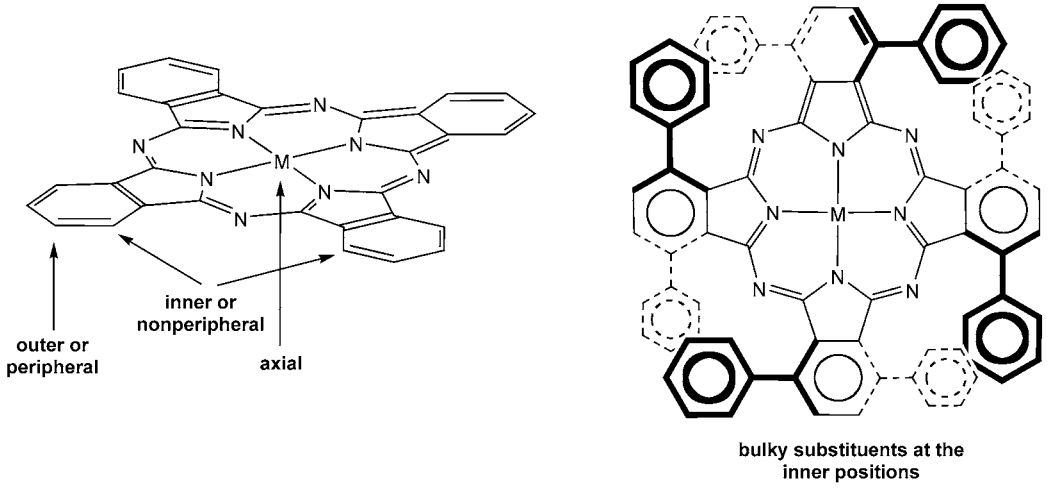

Figure 1. Strategic molecular substitution in Pcs to improve their solubility.

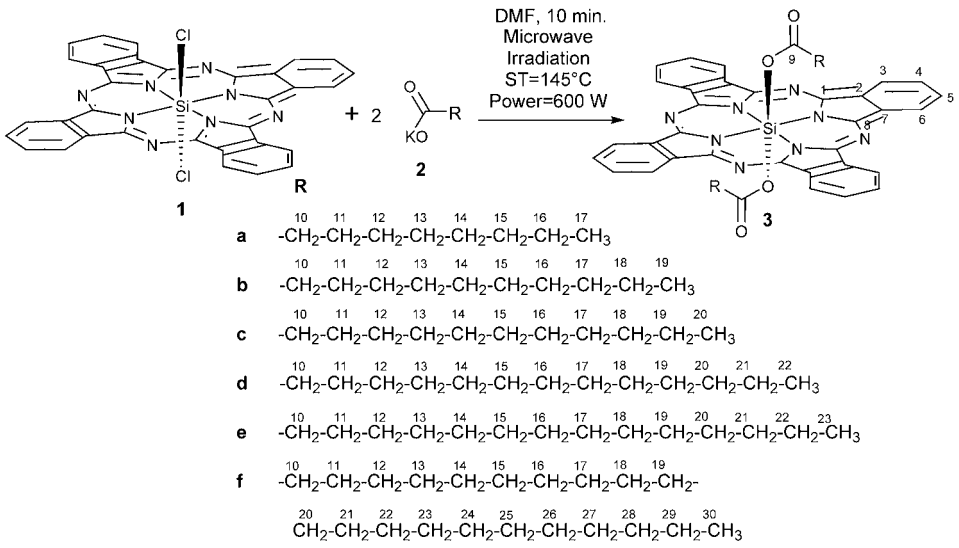

Scheme 1. Synthetic route for the preparation of compounds **3a–3f** and the numbering scheme used in the NMR assignments.

135.7(4) ppm, C-3,6 at $\delta = 131.2(4)$ ppm, C-4,5 at $\delta = 124.0(0)$ ppm and finally the C-9, which corresponds to the silicon ester carbon, at $\delta = 167.4(5)$ ppm. The signals for the carbon atoms in the hydrocarbon tail appear in the range of 35.0 to 14.0 ppm and most of them are specifically affected by induced polarisation by the Pc system. The first six methylenic carbon nuclei exhibited well-resolved signals with chemical shifts as follows: C-10 at $\delta = 34.33(5)$ ppm, C-11 at $\delta = 23.23(5)$ ppm, C-12 at $\delta = 27.43(5)$ ppm, C-13 at $\delta = 28.62(7)$ ppm, C-14 at $\delta = 28.88(13)$ ppm and C-15 at $\delta = 29.40(0)$ ppm. The signals from the middle carbon atoms are more difficult to assign due to signal overlapping. The signals for the last three carbon atoms in each tail were again easily assigned because they are sufficiently separated: $\delta = 32.07(36)$ ppm for the γ position, $\delta = 22.75(8)$ ppm for the β position and $\delta = 14.18(7)$ ppm for the α position.

A literature search for ^{29}Si NMR chemical shifts measured in solution has indicated that compounds containing hexa- and pentacoordinated silicon atoms are somewhat uncommon and therefore their reported NMR data is scarce.[21] For compounds **3a–3f**, the ^{29}Si chemical shifts are at $\delta = -222.60(8)$ ppm. Note that compounds of type **3** possess four nitrogen and two oxygen atoms directly attached to the silicon atom. The chemical shifts for the penta- and/or hexacoordinated silicon atoms are expected to range from $\delta = -127$ to -197 ppm for cationic, anionic and neutral compounds in which the silicon atom is directly attached to two, three, four or six oxygen atoms and with the remaining positions occupied by carbon atoms.[22] Although some other systems appear somewhat deshielded, for example, from $\delta = -20$ to -70 ppm depending on the molecular structures, for purposes of comparison, we are mainly interested in those that show substantial shielding. From the results of previously published studies, it has been proposed that when two oxygen atoms are replaced by CH_3 or Cl substituents marked deshielding arises. In our case, the presence of two less electronegative nitrogen atoms instead of two oxygen atoms results in the most shielded shifts observed so far for hexacoordinated silicon atoms. The resulting signal is thus shifted from the lower limit of $\delta = -197$ ppm, considered above, to approximately $\delta = -222.6$ ppm, a difference of 25.6 ppm. Note that the Pc^{2-} ligand induces substantial shielding at the cavity position.[23] This paper is important as it is the first report of ^{29}Si NMR studies of silicon-containing phthalocyanines. Therefore, the chemical shifts observed for the complexes reported in this contribution stand as the first values that can be used as reference for similar compounds.

X-ray diffraction analysis: The molecular structures of **3a**, **3c**, **3d**, **3e** and **3f** were determined by single-crystal X-ray diffraction studies (Figure 2, Figure 3, Table 1 and Table 2).

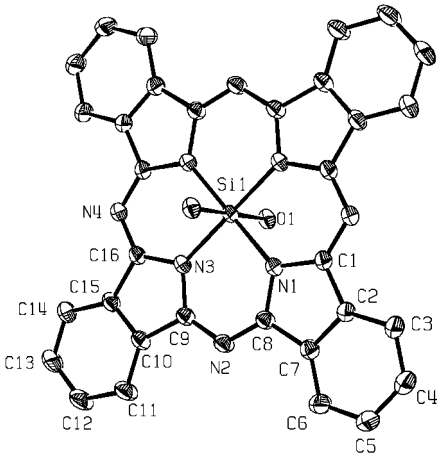

Figure 2. Typical X-ray structure and numbering scheme used for the geometrical variables of $PcSi(O_2CR)_2$.

Note that the numbering schemes used for the X-ray and NMR analyses are different for symmetry reasons. Also, compound **3c** has two different molecules in the asymmetric unit and hence a different numbering scheme is used in this case; the first number corresponds to the molecule and the remaining to the position in the structure, also the mentioned parameters are reported in pairs for this reason. In all cases the silicon atom lies at the centre of an axially distorted octahedron and has a coordination number of six with four nitrogen and two oxygen atoms as neighbours.

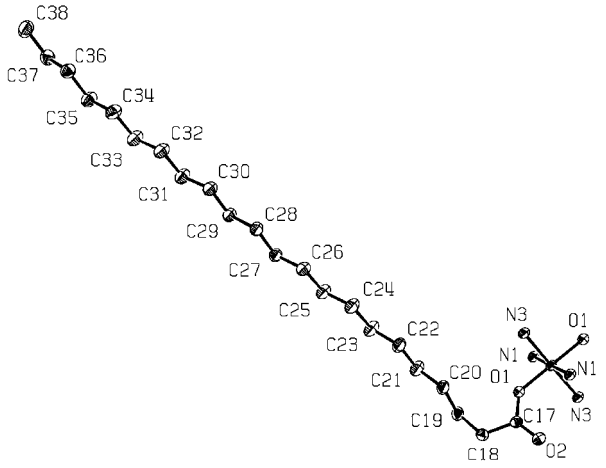

Figure 3. Tail numbering used for compound **3f**.

The two carboxylate fragments attached to the silicon centre have a *trans* configuration and lie above and below the Pc^{2-} ligand with an *anti* orientation. Therefore only half of the molecules were structurally solved due to the presence of an inversion centre. The Si–N distances are 1.9017(18) and 1.9063(15) Å for **3a**, 1.902(2) Å for **3c**, 1.9036(10) and 1.9087(10) Å for **3e** and 1.9008(10) and 1.9092(10) Å for **3f**. The Si–O distances are 1.7487(14) Å for **3a**, 1.7542(18) Å for **3c**, 1.7449(9) Å for **3e** and 1.7467(8) Å for **3f**. These values are similar to those reported for $PcSi(OSiMe_3)_2$,[24] $PcSi(OOCFc)_2$[18b] and $PcSiCl_2$.[25] The C=O and C–O bond lengths are 1.207(2) and 1.324(2) Å for **3a**, 1.198(3) and 1.319(3) Å for **3c**, 1.210(3) and 1.320(3) for **3d**, 1.2065(17) and 1.322(2) for **3e** and 1.2114(16) and 1.3226(15) for **3f**, which indicates that there is no delocalisation in the carboxylate fragment. The N–Si–N bond angles have values of 90.04(7)° for **3a**, 89.95(9)° for **3c**, 89.85(4)° for **3e** and 89.93(4)° for **3f**, which defines a square-planar geometry for the bonded nitrogen and silicon atoms. The O–Si–O bond angle is always 180° demonstrating that there are no significant deformations in the axial positions, whilst the N–Si–O bond angles are close to 90°, again reflecting no significant deformation in the geometry surrounding the silicon atom.

The supramolecular variables that significantly affect the spacing between the Pc planes and therefore the solubility of the compounds are listed in Table 3. The parameter commonly used as a measure of the Pc···Pc spacing is the cofacial Pc···Pc distance,[15b] which, for the present series, exhibits parabolic behaviour, with smaller values, 11.099 and 11.8258 Å, for **3a** and **3e**, and larger ones, 19.0296 and 12.936 Å, for **3c** and **3d**, respectively (compound **3c** is particularly interesting and therefore it has been analysed in more detail since it is the only example for which two molecules are present in the asymmetric unit). For even longer hydrocarbon tails, for example, **3f**, the spacing is approximately 4.5 Å larger than the statistical median of the other measured quantities.

The conformation of the Pc^{2-} ligand is another supramolecular variable that changes significantly depending on the length of the hydrocarbon tail (Table 3). The conformations of the Pc^{2-} ligands are described as follows: compounds **3a** and **3f**, the compounds with the shortest and longest tails, adopt half-waved conformations, the conformations the Pc moiety of **3c** and **3e** are planar, and **3d**, the compound with the middle-sized tail, is the only example to adopt a completely waved Pc^{2-} conformation. Unfortunately the observed behaviour is not easily understood.

Table 1. Crystallographic data[a] for compounds **3a**, **3c**, **3d**, **3e** and **3f**.

Compound	**3a**	**3c**	**3d**	**3e**	**3f**
chemical formula	$C_{50}H_{50}N_8O_4Si$	$C_{56}H_{62}N_8O_4Si$	$C_{60}H_{70}N_8O_4Si$	$C_{62}H_{74}N_8O_4Si$	$C_{76}H_{102}N_8O_4Si$
formula weight	885.08	939.24	995.33	1023.38	1219.74
unit cell dimensions					
a [Å]	9.044(5)	9.0041(3)	9.102(5)	11.0300(2)	9.1750(2)
b [Å]	11.099(5)	15.5340(5)	11.571(5)	11.8258(2)	11.8790(2)
c [Å]	11.678(5)	19.0296(6)	12.936(5)	11.7870(3)	16.5900(3)
α [°]	97.456(5)	105.7650(10)	93.940(5)	90.1070(10)	102.481(1)
β [°]	98.112(5)	100.6540(10)	93.770(5)	107.0880(10)	91.802(1)
γ [°]	106.408(5)	93.849(2)	100.590(5)	109.1080(10)	102.328(1)
volume [Å^3]	1095.3(9)	2497.93(14)	1331.8(11)	1380.43(5)	1718.99(6)
Z	1	2	1	1	1
$\rho_{calcd.}$ [g cm^{-3}]	1.296	1.249	1.241	1.231	1.178
μ [mm^{-1}]	0.110	0.102	0.100	0.098	0.089
θ [°]	2.58 to 27.43	3.46 to 27.53	3.51 to 26.29	3.54 to 27.46	3.42 to 27.50
collected reflections	8106	38264	9052	21379	13142
ind. reflections [R(int.)]	4944[0.028]	11341[0.107]	5222[0.063]	6262[0.082]	7691[0.019]
completeness to θ [°,%]	27.43,99.0	27.53,98.6	26.29,96.9	27.46,98.9	27.50,97.2
data/restraints/param.	4944/6/358	11341/0/797	5222/108/438	6262/0/488	7691/0/608
GOOF	1.032	1.011	1.017	1.026	1.027
R [%]	5.67	6.57	6.61	4.57	4.35
wR (all data) [%]	16.29	17.12	17.15	12.63	11.82
ρ_{min} [e Å^{-3}]	−0.389	−0.241	−0.339	−0.317	−0.235
ρ_{max} [e Å^{-3}]	0.811	0.275	0.289	0.469	0.192

[a] All the compounds exhibited a triclinic crystal system and a $P\bar{1}$ space group.

Table 2. Selected bond lengths, bond angles and internal/external diameters of compounds **3a**, **3c**, **3d**, **3e** and **3f**.

Compound	**3a**	**3c**	**3d**	**3e**	**3f**
bond lengths [Å]					
N−Si	1.9017(18)	1.902(2)	1.909(2)	1.9036(10)	1.9008(10)
N−Si	1.9063(15)	1.902(2)	1.896(2)	1.9087(10)	1.9092(10)
Si−O	1.7487(14)	1.7542(18)	1.746(2)	1.7449(9)	1.7467(8)
O−C	1.324(2)	1.319(3)	1.320(3)	1.322(2)	1.3226(15)
C=O	1.207(2)	1.198(3)	1.210(3)	1.2065(17)	1.2114(16)
bond angles [°]					
N-Si-N	90.04(7)	89.95(9)	90.04(9)	89.85(4)	89.93(4)
O-Si-O	180.0(8)	180.0(4)	180.00(1)	180.00(6)	180.0(6)
N-Si-O	93.87(6)	92.81(8)	86.71(9)	86.58(4)	86.69(4)
N-Si-O	92.65(6)	93.20(9)	86.65(9)	86.94(4)	93.34(4)
Si-O-C	134.34(12)	135.36(17)	134.69(19)	135.05(9)	134.44(8)
O-C=O	124.57(17)	124.4(3)	124.5(3)	124.54(13)	124.50(12)
O-C-C	111.43(18)	113.3(3)	113.5(3)	112.35(12)	113.64(11)
O=C-C	124.00(18)	122.3(3)	122.0(3)	123.08(13)	121.87(12)
cavity diameter [Å]					
$2\times d$(N−Si)	3.813	3.803	3.818	3.817	3.818
$2\times d$(N−Si)	3.803	3.803	3.792	3.807	3.802
external diameter [Å]					
$2\times d$(Si–C4)	13.038	13.041	13.004	13.058	13.028
$2\times d$(Si–C5)	13.034	13.047	13.018	13.034	13.046
$2\times d$(Si–C12)	13.041	13.018	13.048	13.055	13.059
$2\times d$(Si–C13)	13.043	13.010	13.030	13.054	13.047

The conformation of the tail is even more difficult to rationalise since it is known that some conformational changes are likely to occur depending on the crystallisation conditions.[20b] The spacers induce waved conformations in compounds **3a** (with nine carbon atoms in the tail), **3d** (with 12 carbon atoms) and **3f** (with 22 carbon atoms). The presence of two different molecules in the asymmetric unit in compound **3c** gives rise to a ruffled or twisted conformation whilst the hydrocarbon tail in compound **3e** accommodates itself in a perfectly aligned fashion (Table 3).

Other important factors that influence the spacing between the Pc planes are the σ–σ and π–π Pc–Pc interactions, which mainly depend on the efficiency of the axial substituents to create some space between the Pc planes (Table 3). In this regard, compound **3a** does not exhibit the expected σ interactions, but only certain π forces, as can be deduced from the following data: d(N4–C3) = 3.404, d(C4–C16) = 3.425, d(C4–C15) = 3.507, d(C5–C15) = 3.443 and d(C4–C14) = 3.537 Å. The σ–σ Pc–Pc interactions are perpendicular in **3c** (there are two different molecules in the asymmetric unit of **3c**

Table 3. Supramolecular contacts, shape, spacer behaviour and π–π and σ–σ Pc–Pc packing for **3a**, **3c**, **3d**, **3e** and **3f**.

Compound	**3a**	**3c**[a]	**3d**	**3e**	**3f**
Cofacial Pc···Pc distance [Å]					
lattice parameter	$b = 11.099$	$a = 9.0041$ $c = 19.0296$	$c = 12.936$	$b = 11.8258$	$c = 16.5900$
Pc conformation	half-waved	plain	waved	plain	half-waved
tail conformation	waved	ruffled/twisted	waved	aligned	waved
tail orientation	parallel	parallel	parallel	parallel	parallel
lateral view	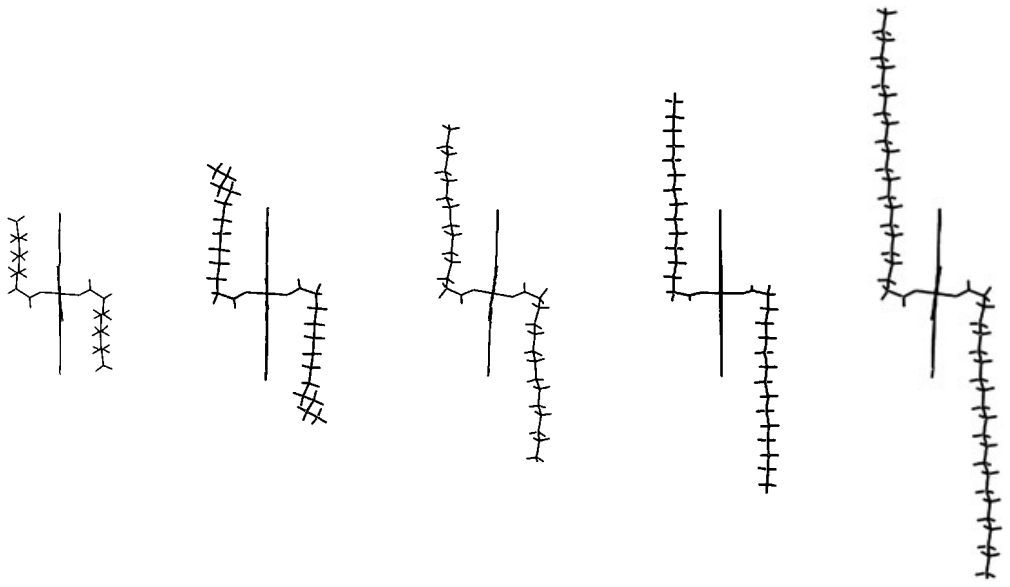				

Table 3. (Continued)

Compound	3a	3c[a]	3d	3e	3f
Pc plane view	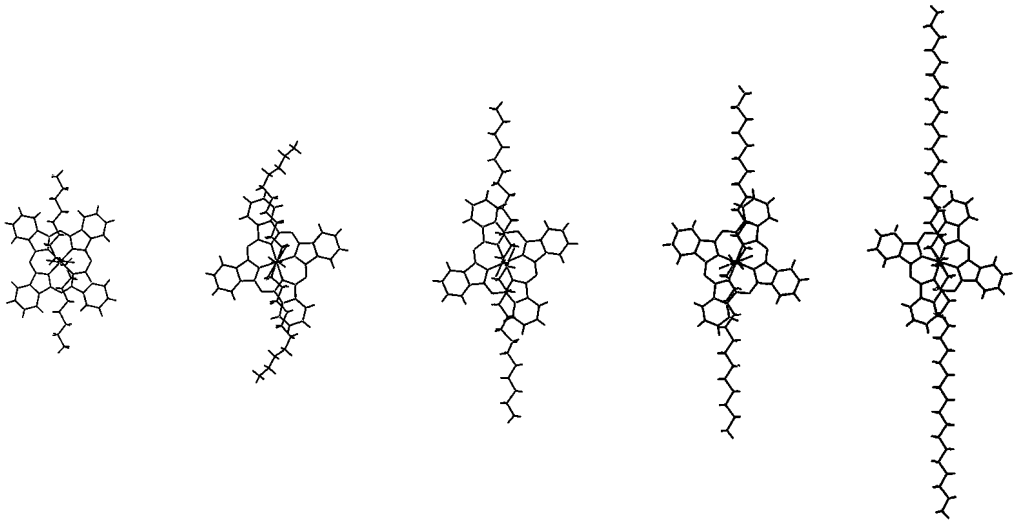				
σ–σ Pc–Pc interaction [b]	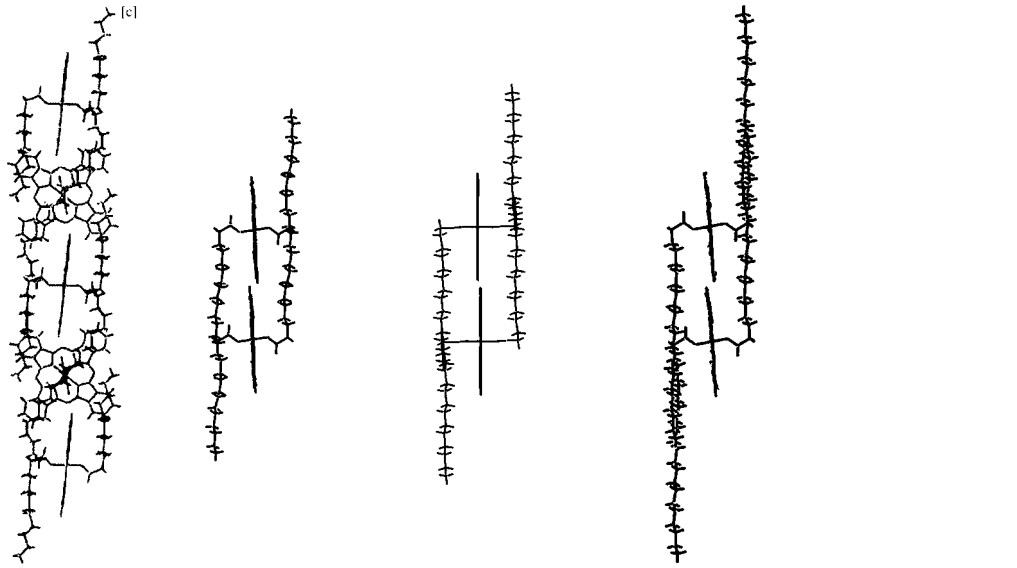 [c]				
π–π Pc–Pc interaction	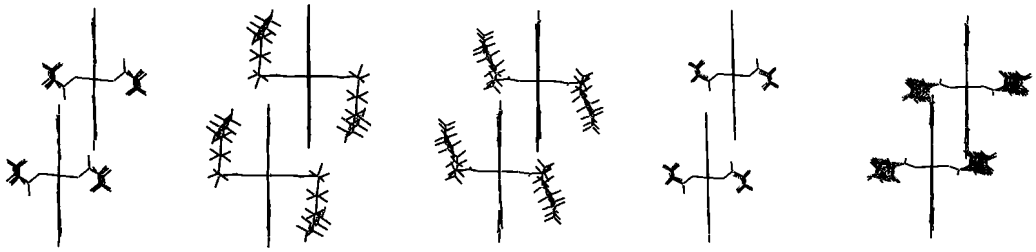				

[a] Because there are two different Pc molecules in the asymmetric unit, there are also two cofacial Pc spacing distances for this supramolecular structure, which are different from the others. [b] The expected σ–σ Pc–Pc interaction is not present owing to the shorter length of the hydrocarbon tail. [c] Owing to perpendicular σ–σ Pc–Pc interactions, a helical structure is present. Note that this is the only example in which two different molecules are present in the crystallographic cell.

and hence a different numbering scheme is used in this case; the first number corresponds to the molecule and the remaining to the position in the structure), and a helical structure is present, with d(N12–H39) = 2.759, d(N12–H40) = 2.857, d(N22–H4) = 2.852 and d(N22–H5) = 2.776 Å. The π–π Pc–Pc interactions for **3c** give d(C21–C214) = 3.536, d(C22–C213) = 3.478, d(C27–C213) = 3.501, d(C23–C212) = 3.701, d(C24–C212) = 3.507, d(C22–C213) = 3.478, d-

(C22–C214) = 3.476, *d*(C23–C215) = 3.674, *d*(C23–C210) = 3.644, *d*(C23–C211) = 3.667, *d*(C24–C211) = 3.474, *d*(C24–C212) = 3.507, *d*(C25–C212) = 3.534 and *d*(C27–C213) = 3.501 Å. Compounds **3d**, **3e** and **3f** behave in a common way, exhibiting equivalent interactions at equivalent atomic positions. The σ–σ Pc–Pc interactions present in compound **3d** result in *d*(H5–H6) = 2.465, *d*(H6–H6) = 2.198, *d*(N2–H5) = 3.304, *d*(H5–H11) = 2.583 and *d*(H4–H11) = 2.812 Å. The π–π Pc–Pc interactions for **3d** give *d*(C3–N4) = 3.479, *d*(C3–C16) = 3.485, *d*(C4–C16) = 3.623, *d*(C4–C15) = 3.548, *d*(C5–C15) = 3.775, *d*(C5–C14) = 3.794 and *d*(C6–C14) = 3.807 Å. The σ–σ Pc–Pc interactions in compound **3e** give *d*(H3–H3) = 2.161, *d*(H3–H4) = 2.551, *d*(N4–H4) = 3.481, *d*(H4–H14) = 2.497 and *d*(H5–H14) = 3.100 Å. The π–π Pc–Pc interactions in **3e** give *d*(C6–C6) = 3.488, *d*(C13–C15) = 3.535, *d*(C14–C15) = 3.665, *d*(C14–C14) = 3.744 and *d*(C13–C14) = 3.852 Å. Finally, the σ–σ Pc–Pc interactions in compound **3f** give *d*(H3–H4) = 2.613, *d*(H3–H3) = 2.247, *d*(N4–H4) = 3.370, *d*(H4–H14) = 2.594 and *d*(H5–H14) = 2.897 Å, and for the corresponding π–π Pc–Pc interactions, *d*(C3–C12) = 3.968, *d*(C3–C11) = 3.835, *d*(C4–C11) = 3.804, *d*(C4–C10) = 3.859, *d*(C5–C10) = 3.535, *d*(C5–C15) = 3.760, *d*(C6–C9) = 3.507 and *d*(C6–N2) = 3.537 Å.

In the X-ray analysis of the supramolecular structures (Figure 4, Figure 5 and Figure 6), the intramolecular distances from C-18 (the first methylenic carbon atom of each individual tail and the reference position) to each of the first eight carbon atoms in the hydrocarbon tail, referred to as the radial distance, rD_{Pc} [Å], were measured (Table 4). Moreover, the distances between the averaged plane constituted by the Pc ligand and again each of the first eight methylenic carbon atoms in the tail, referred to as the distance from the Pc to the tail, $D_{Pc\text{-}Tail}$ [Å], are summarised in Table 4. By plotting both series of data a useful graph was obtained (Figure 4) which reveals the dynamic intrasupramolecular behaviour of the tails in the crystalline solid-state structures. Compound **3a** has a minimum tail distance from the Pc plane of 5.0 Å, corresponding to C-22. For compounds **3a** and **3c**, the distances of all the positions (C-18 to C-25) analysed from the Pc plane are nonalternating, but show opposite trends; for example, **3a** has a tail that tends to become more distant from the Pc plane beyond the C-22 position, like in compounds **3d**, **3e** and **3f**. Compound **3c** is the only example in which the methylenic units become more proximal to the Pc system beyond the C-22 position. For compounds **3d**, **3e** and **3f**, the distances of all the posi-

Table 4. Selected intramolecular distances and Pc plane deviations, as well as selected ^{1}H NMR chemical shifts for compounds **3a**, **3c**, **3d**, **3e** and **3f**.

Compound	**3a**	**3c**	**3d**	**3e**	**3f**	Average
radial distance, rD_{Pc} [Å]						
reference C-18	0	0	0	0	0	0
C-18 to C-19	1.510	1.513	1.509	1.524	1.517	1.515
C-18 to C-20	2.539	2.535	2.529	2.549	2.552	2.541
C-18 to C-21	3.880	3.877	3.888	3.905	3.908	3.892
C-18 to C-22	5.052	5.090	5.053	5.105	5.078	5.076
C-18 to C-23	6.376	6.389	6.335	6.416	6.408	6.385
C-18 to C-24	7.547	7.626	7.625	7.651	7.604	7.611
C-18 to C-25	8.793	8.873	8.633	8.951	8.911	8.832
hydrocarbon tail to Pc plane distance, $D_{Pc\text{-}Tail}$ [Å]						
Pc ring to C-18	4.006	4.104	4.096	4.086	4.103	–
Pc ring to C-19	3.882	4.145	4.115	4.108	4.124	–
Pc ring to C-20	3.738	3.979	3.827	3.869	3.858	–
Pc ring to C-21	3.661	3.959	3.924	3.937	3.984	–
Pc ring to C-22	3.601	3.846	3.889	3.772	3.917	–
Pc ring to C-23	3.662	3.744	4.140	3.938	4.165	–
Pc-ring to C-24	3.686	3.574	4.346	3.765	4.158	–
Pc-ring to C-25	3.836	3.289	4.709	4.022	4.506	–
^{1}H NMR chemical shifts [ppm]						average
H-10	−0.64	−0.54	−0.61	−0.61	−0.64	−0.608
H-11	−0.96	−0.86	−0.93	−0.93	−0.95	−0.926
H-12	−0.74	−0.66	−0.72	−0.72	−0.74	−0.716
H-13	0.06	0.14	0.08	0.08	0.08	0.088
H-14	0.54	0.60	0.55	0.55	0.54	0.556
H-15	0.81	0.88	0.84	0.83	0.83	0.838
H-16	1.08	1.10	1.06	1.06	1.06	1.072
^{1}H NMR chemical shifts [δ] for the free fatty acids using the same numbering scheme as that used in this work [ppm]			$\Delta\delta$ between the averaged three compounds and the free fatty acid form [ppm] (upper and lower limits)			
H-10		2.40–2.20			3.01–2.81	
H-11		1.70–1.50			2.62–2.43	
H-12		1.35–1.10			2.09–1.82	
H-13		1.32–1.24			1.23–1.15	
H-14		1.32–1.24			0.76–0.68	
H-15		1.32–1.24			0.48–0.40	
H-16		1.32–1.24			0.25–0.17	

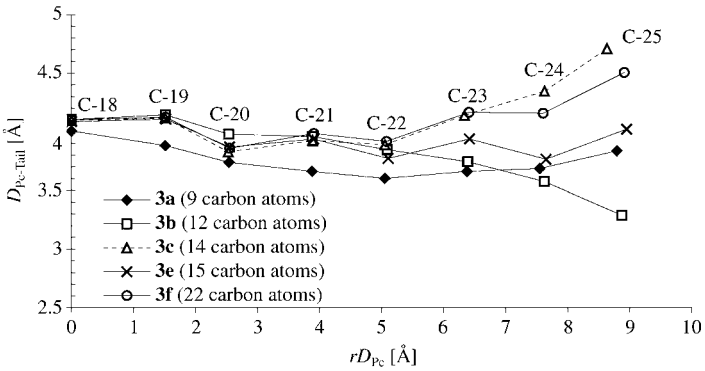

Figure 4. Spacing between the Pc ligand and tail, $D_{Pc\text{-}Tail}$, versus the radial distance, rD_{Pc}, from X-ray analysis data.

tions analysed (C-18 to C-25) from the Pc plane alternate, as is evident from Figure 4.

Furthermore, the effect of the Pc currents on the systems under study was evaluated by a raw correlation between the ^{1}H NMR chemical shifts, δ [ppm], for H-10 to H-16 (Table 4, Figure 5) and the corresponding radial distances,

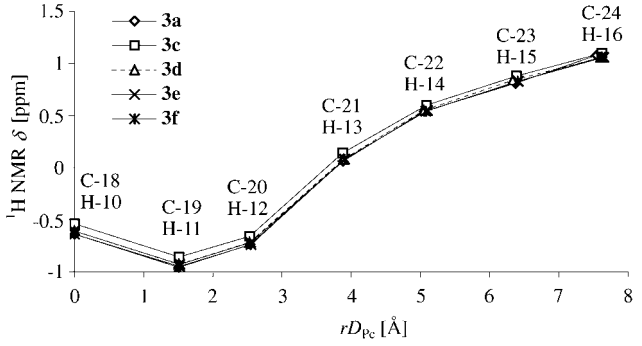

Figure 5. ^{1}H NMR chemical shifts (δ) versus rD_{Pc} as a measure of the effect of Pc currents.

rD_{Pc} [Å], for C-18 to C-24 (Table 4, Figure 5). There is a clear decrease in shielding as the position of the hydrogen atom moves away from the centre of the Pc system. This is more conspicuous in the first three positions due to the additional effects of a normal carboxylate moiety at the α, β and γ positions. The chemical shifts for these three positions are in the range of $\delta = 2.40$–2.20, 1.70–1.50 and 1.35–1.10 ppm, respectively, as reported for octanoic through to docosanoic acid.[26] The remaining ^{1}H NMR signals, which remain constant throughout the fatty acids, are between $\delta =$ 1.32–1.24 ppm.[26] The shielding observed (taking the previously reported chemical shifts for the free acid forms as reference) in the Pc system for compounds of type **3** are in the range of $\delta = 2.99$–2.87 ppm for the α position, $\delta = 2.68$–2.52 ppm for the β position, and finally $\delta = 2.07$–1.84 ppm for the γ position. Farren et al.[27], in a previous study, reported a comparable graph that showed quite similar shielding behaviour. In this case, the compounds reported were the PcSi[O_2C-$(CH_2)_n$-Ar]$_2$ esters. Also, in pioneering research by Kenney and co-workers on MPc and MPorph (M = Si and Ge) systems, radial shielding was observed in axial hydrocarbon-substituted phthalocyanines-silanols.[28,29]

In any event, a detailed study was performed to take into account the radial decrease in polarisation along the Pc^{2-} ligand. The net shielding loss can be derived from the graph of $\Delta\delta$ [ppm] (obtained from both δ values) for the H-10 to H-16 positions of $HO_2C(CH_2)_nCH_3$ and PcSi-[$O_2C(CH_2)_nCH_3$]$_2$ (**3**) (Table 4) versus the rD_{Pc} [Å] values for C-18 to C-24 of PcSi[$O_2C(CH_2)_nCH_3$]$_2$ (Figure 6). This

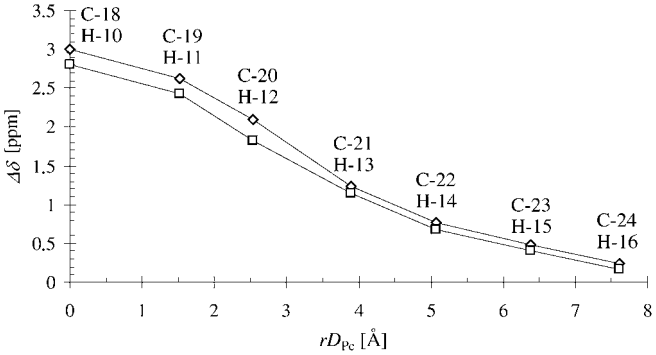

Figure 6. $\Delta\delta$ versus rD_{Pc} to evaluate the net shielding loss along the Pc^{2-} ligand.

graph allows the net radial shielding of the SiPc moiety to be obtained at a mean distance of 3.85 Å from the Pc^{2-} ligand, where long chains lie above (or below) the Pc Plane. The recently reported zero ring-current effect between the α and β Pc sites[30] was not directly confirmed in this work because of substantial overlapping of the remaining signals, which prevented the chemical shifts of the hydrogen atoms beyond H-17 from being plotted in Figure 6. This plot and equations derived from it are thus sustained and therefore important since the carboxylate moiety fixes the orientation of the tail parallel to the Pc plane, as evidenced by the standard deviation of the ^{1}H NMR chemical shifts across the whole series. As there are two ^{1}H NMR limits to the reported values, two linear equations were derived from this analysis. The upper-limit equation is $\Delta\delta = -0.373 \cdot rD_{Pc} + 2.791$ with $R^2 = 0.9725$, with a maximum shielding of $\Delta\delta =$ 2.79 ppm at $rD_{Pc} = 0$ and the shielding effect, $\Delta\delta = 0$, vanishes at $rD_{Pc} = 7.48$ Å instead of 6.0 Å, as previously reported.[30] The lower-limit equation is $\Delta\delta = -0.3951 \cdot rD_{Pc} + 3.0179$ with $R^2 = 0.9679$, with a maximum shielding of $\Delta\delta =$ 3.02 ppm at $rD_{Pc} = 0$ and the shielding effect, $\Delta\delta = 0$, vanishes at $rD_{Pc} = 7.64$ Å. The latter values are considered to occur at the 6th methylenic group, at approximately 4 angstroms below/above the Pc plane. This discrepancy in the observed zero ring-current-effect zone supports the importance attributed to the effect of the central metal as well as the chemical structure of the axial substituents,[30] which needs to be analysed further with more Pc systems. This contribution

should also be useful in future X-ray/NMR phthalocyanine characterisations.

Conclusions

trans-Phthalocyaninesilicon(IV) dichloride can be transformed in moderate yields to *trans*-phthalocyaninesilicon(IV) dicarboxylates through a microwave-assisted reaction.

The ^{1}H and ^{13}C NMR spectra of these silicon(IV)-dicarboxylates revealed that Pc currents, particularly up to the fifth/sixth methylene position, affect the chemical shifts and also the spin-rotational relaxation mainly for the first (α) methylene position. The values of the ^{29}Si NMR chemical shifts measured in $CDCl_3$ are indicative of hexacoordinated silicon(IV) atoms, and are, until now, the most shielded chemical shifts recorded for silicon nuclei in nonalloy compounds in solution. In addition this is the first time that ^{29}Si chemical shifts have been reported for SiPc systems. The COOSi bands in the IR spectra indicate normal σ bonding between the carboxylic oxygen and the silicon atoms.

X-ray structure analysis of the *trans*-phthalocyaninesilicon(IV) dicarboxylate compounds showed that the COOSi moieties are positioned *trans* to the Pc^{2-} ligand and confirmed that the silicon atom has a coordination number of six and thus an octahedral geometry. The supramolecular contacts found within the crystallographic lattices are mainly $\pi\cdots\pi$- and $\sigma\cdots\sigma$-type interactions. As these intermolecular interactions modify the conformations of the tail and induce slight deformations in the Pc ligands, they can have a significant effect, depending on the length of the hydrocarbon tail, on the overall supramolecular shape, which affects the solubility of the compounds. Long tails make a bigger contribution to the spacing and this of course enhances their solubility but their 3D structure cannot be analysed in a simple way through geometrical parameters.

Based on the X-ray data, the distance between the Pc ligand and the hydrocarbon tails is a minimum at the fifth methylenic group of the chain, which indicates that there is a strong interaction between the two moieties. This directly influences the supramolecular behaviour since the spacing variable indicates that the C_{22} chain is the better spacing group. Nevertheless, for shorter chains the behaviour is parabolic with C_{12} the optimum spacer group.

The NMR and X-ray data have allowed the net shielding effect in a radial distribution along the Pc ligand to be derived; the derived equations have allowed the loss of radial shielding in Pc systems to be calculated at an approximate distance of 4 Å from the Pc ligand.

Experimental Section

Fatty acids, dicyanobenzene, silicon tetrachloride, potassium hydroxide and quinoline were purchased from Aldrich Co. DMF, dichloromethane, hexanes and methanol were purchased as reagent grade from Fermont. All reactions and operations were carried out under atmospheric conditions unless stated otherwise. Quinoline was freshly distilled before use. $PcSiCl_2$ (**1**) was prepared according to the previously reported microwave methodology.[25]

Instrumentation: NMR experiments were performed with a JEOL ECLIPSE-400 spectrometer. ^{1}H and ^{13}C chemical shifts [ppm] are reported relative to internal $SiMe_4$ (TMS) ($\delta_H=0$, $\delta_C=0$, $\delta_{Si}=0$). Coupling constants are quoted in Hz. The ^{29}Si NMR experiments were carried out by inverse gated decoupling with a relaxation delay of 2.5 s to increase the intensity of the singlet signals of silicon with octahedral geometry. The IR spectra were recorded in the range 4000–400 cm^{-1} with a Bruker Tensor-27 FT-IR spectrometer using KBr pellets. UV/Vis spectra were obtained with a Lambda 35 Perkin-Elmer spectrometer. Elemental analyses were obtained with a CHNO/S Perkin-Elmer apparatus.

Preparation of $PcSiCl_2$: Compound **1** was prepared following the method reported by Davies et al.[25]

Preparation of fatty acid salts: General procedure for the preparation of **2a**: Pelargonic acid **1a** (10.0 g, 63 mmol) and potassium hydroxide (3.546 g, 63 mmol) in methanol (100 mL) were refluxed in a 250 mL flask for 2 h. The solvent was then removed under reduced pressure and the remaining solid was washed twice with 20 mL portions of chloroform/heptanes (1:6) to yield **2a** (9.678 g, 49 mmol, 78%) as a white amorphous solid.

Equimolecular quantities of starting materials gave compounds **2b–2f** in yields of 87% for **2b**, 86% for **2c**,[20] 81% for **2d**,[20] 83% for **2e** and 92% for **2f**.

Preparation of compounds 3a–3f by microwave irradiation: General procedure for compound **3a**: $PcSiCl_2$ (**1**) (0.5 g, 0.82 mmol) and **2a** (0.321 g, 1.64 mmol) were added to a 100 mL reaction flask and the solution was heated for 10 minutes in the microwave reactor with a power supply of 600 W and a temperature set previously at 145 °C.[20] After completing the reaction, the product was rinsed with a mixture of methanol and bidistilled water (100 mL, 1:1). The precipitate was filtered and washed at least five times with a mixture of methanol and bidistilled water (3:1). The resulting dark blue powder was identified as **3a** (0.294 g, 0.34 mmol, 42%). The other compounds in the series were obtained by following the same procedure.

Compound $PcSi[O_2C(CH_2)_7CH_3]_2$ (3a): Blue powder, yield 42%, m.p. >264 °C (decomp). IR (KBr pellets): $\tilde{\nu}=2950$, 2921, 2848, 1692, 1620, 1528, 1474, 1430, 1336, 1122, 1080, 1063, 761, 737 cm^{-1}. UV ($CHCl_3$): $\lambda=$ 291, 325, 367, 370, 616, 653, 670, 697 nm. ^{1}H NMR: $\delta=8.38$ (dd, $J_o=5.5$, $J_m=2.6$ Hz, H-3,6), 9.69 (dd, $J_o=5.5$, $J_m=2.6$ Hz, H-4,5), −0.64 (t, $J=$ 7.3 Hz, H-10), −0.96 (q, $J=7.3$ Hz, H-11), −0.74 (q, $J=7.3$ Hz, H-12), 0.06 (q, $J=7.3$ Hz, H-13), 0.54 (q, $J=7.3$ Hz, H-14), 0.81 (q, $J=7.3$ Hz, H-15), 1.08 (sextet, $J=7.3$ Hz, H-16), 0.80 ppm (t, $J=7.3$ Hz, H-17); ^{13}C NMR: $\delta=150.0$ (C-1,8), 135.6 (C-2,7), 131.2 (C-3,6), 124.0 (C-4,5), 167.4 (C-9), 34.3 (C-10), 23.2 (C-11), 27.4 (C-12), 28.5 (C-13), 28.6 (C-14), 31.6 (C-15), 22.6 (C-16), 14.1 ppm (C-17); ^{29}Si NMR: $\delta=-222.7$ ppm; elemental analyses calcd (%) for $C_{50}H_{50}N_8O_4Si$: C 70.23, H 5.89, N 13.10; found: C 69.85, H 6.01, N 13.04. Suitable crystals for the X-ray diffraction study were obtained in a 7:2 solution of hexanes and dichloromethane.

Compound $PcSi[O_2C(CH_2)_9CH_3]_2$ (3b): Blue powder, yield 64%, m.p. 204–205 °C. IR (KBr pellets): $\tilde{\nu}=2957$, 2923, 2852, 1685, 1610, 1527, 1459, 1430, 1336, 1289, 1267, 1121, 1082, 912, 761, 738 cm^{-1}; UV ($CHCl_3$): $\lambda=$ 292, 340, 365, 372, 615, 653, 676, 702 nm; ^{1}H NMR: $\delta=8.39$ (dd, $J_o=5.5$, $J_m=3.0$ Hz, H-3,6), 9.73 (dd, $J_o=5.5$, $J_m=3.0$ Hz, H-4,5), −0.56 (t, $J=$ 7.0 Hz, H-10), −0.88 (q, $J=7.0$ Hz, H-11), −0.67 (q, $J=7.0$ Hz, H-12), 0.13 (q, $J=7.0$ Hz, H-13), 0.59 (q, $J=7.0$ Hz, H-14), 0.87 (q, $J=7.0$ Hz, H-15), 1.10 (q, $J=7.0$ Hz, H-16,), 1.20 (q, $J=7.0$ Hz, H-17), 1.31 (sextet, $J=7.0$ Hz, H-18), 0.94 ppm (t, $J=7.0$ Hz, H-19); ^{13}C NMR: $\delta=150.1$ (C-1,8), 135.7 (C-2,7), 131.2 (C-3,6), 124.0 (C-4,5), 167.4 (C-9), 34.4 (C-10), 23.3 (C-11), 27.5 (C-12), 28.7 (C-13), 29.0 (C-14), 29.4 (C-15), 29.3 (C-16), 32.0 (C-17), 22.8 (C-18), 14.2 ppm (C-19); ^{29}Si NMR: $\delta=$ −222.5 ppm; elemental analyses calcd (%) for $C_{54}H_{58}N_8O_4Si$: C 71.18, H 6.42, N 12.30; found: C 71.44, H 6.60, N 12.24.

Compound $PcSi[O_2C(CH_2)_{10}CH_3]_2$ (3c): Blue powder, yield 48%, m.p. > 212 °C (decomp). IR (KBr pellets): $\tilde{\nu}=2974$, 2920, 2855, 1678, 1602, 1520, 1464, 1431, 1336, 1288, 1165, 1077, 1064, 913, 785, 762, 702 cm^{-1}; UV

($CHCl_3$): $\lambda = 294$, 330, 342, 367, 618, 654, 674, 699 nm; ^{1}H NMR: $\delta = 8.39$ (dd, $J_o = 5.8$, $J_m = 2.9$ Hz, H-3,6), 9.74 (dd, $J_o = 5.8$, $J_m = 2.9$ Hz, H-4,5), −0.54 (t, $J = 7.0$ Hz, H-10), −0.86 (q, $J = 7.0$ Hz, H-11), −0.66 (q, $J = 7.0$ Hz, H-12), 0.14 (q, $J = 7.0$ Hz, H-13), 0.60 (q, $J = 7.0$ Hz, H-14), 0.88 (q, $J = 7.0$ Hz, H-15), 1.10 (q, $J = 7.0$ Hz, H-16), 1.26 (q, $J = 7.0$ Hz, H-17), 1.32 (q, $J = 7.0$ Hz, H-18), 1.35 (sextet, $J = 7.0$ Hz, H-19), 0.96 ppm (t, $J = 7.0$ Hz, H-20); ^{13}C NMR: $\delta = 150.1$ (C-1,8), 135.7 (C-2,7), 131.3 (C-3,6), 124.0 (C-4,5), 167.4 (C-9), 34.4 (C-10), 23.3 (C-11), 27.5 (C-12), 28.7 (C-13), 29.0 (C-14), 29.4 (C-15), 29.6 (C-16), 29.5 (C-17), 32.0 (C-18), 22.8 (C-19), 14.3 ppm (C-20); ^{29}Si NMR: $\delta = -222.5$ ppm; elemental analyses calcd (%) for $C_{56}H_{62}N_8O_4Si$: C 71.61, H 6.65, N 11.93; found: C 71.87, H 6.72, N 12.16. Suitable crystals for the X-ray diffraction study were obtained in a 2:1 solution of hexanes and dichloromethane.

Compound PcSi[$O_2C(CH_2)_{12}CH_3$]$_2$ (3d): Blue powder, yield 51%, m.p. 151–153 °C. IR (KBr pellets): $\tilde{\nu} = 2970$, 2923, 2849, 1681, 1613, 1528, 1467, 1431, 1337, 1288, 1165, 1125, 1082, 1064, 913, 785, 761, 698 cm^{-1}. UV ($CHCl_3$): $\lambda = 297$, 323, 369, 372, 620, 655, 672, 702 nm; ^{1}H NMR: $\delta = 8.38$ (dd, $J_o = 5.9$, $J_m = 2.9$ Hz, H-3,6), 9.70 (dd, $J_o = 5.9$, $J_m = 2.9$ Hz, H-4,5), −0.61 (t, $J = 6.8$ Hz, H-10), −0.93 (q, $J = 6.8$ Hz, H-11), −0.72 (q, $J = 6.8$ Hz, H-12), 0.08 (q, $J = 6.8$ Hz, H-13), 0.55 (q, $J = 6.8$ Hz, H-14), 0.84 (q, $J = 6.8$ Hz, H-15), 1.06 (q, $J = 6.8$ Hz, H-16), 1.18 (q, $J = 6.8$ Hz, H-17), 1.30–1.24 (m, H-18), 1.30–1.24 (m, H-19), 1.30–1.24 (m, H-20), 1.33 (sextet, $J = 6.8$ Hz, H-21), 0.93 ppm (t, $J = 6.8$ Hz, H-22); ^{13}C NMR: $\delta = 150.1$ (C-1,8), 135.7 (C-2,7), 131.2 (C-3,6), 124.0 (C-4,5), 167.3 (C-9), 34.3 (C-10), 23.2 (C-11), 27.4 (C-12), 28.6 (C-13), 28.9 (C-14), 29.4 (C-15), 29.6 (C-16), 29.5 (C-17), 29.7 (C-18), 29.7 (C-19), 32.0 (C-20), 22.8 (C-21), 14.2 ppm (C-22); ^{29}Si NMR: $\delta = -222.6$ ppm; elemental analyses calcd (%) for $C_{60}H_{70}N_8O_4Si$: C 72.40, H 7.09, N 11.26; found: C 72.65, H 7.24, N 11.38. Suitable crystals for the X-ray diffraction study were obtained in a 5:2 solution of hexanes and dichloromethane.

Compound PcSi[$O_2C(CH_2)_{13}CH_3$]$_2$ (3e): Blue powder, yield 67%, m.p. 171–173 °C . IR (KBr pellets): $\tilde{\nu} = 2960$, 2925, 2849, 1686, 1611, 1527, 1460, 1430, 1353, 1336, 1288, 1269, 1123, 1082, 1061, 913, 761, 738, 702 cm^{-1}. UV ($CHCl_3$): $\lambda = 295$, 330, 368, 612, 652, 678, 700 nm. ^{1}H NMR: $\delta = 8.37$ (dd, $J_o = 5.8$, $J_m = 2.9$ Hz, H-3,6), 9.70 (dd, $J_o = 5.8$, $J_m = 2.9$ Hz, H-4,5), −0.61 (t, $J = 6.8$ Hz, H-10), −0.93 (q, $J = 6.8$ Hz, H-11), −0.72 (q, $J = 6.8$ Hz, H-12), 0.08 (q, $J = 6.8$ Hz, H-13), 0.55 (q, $J = 6.8$ Hz, H-14), 0.83 (q, $J = 6.8$ Hz, H-15), 1.06 (q, $J = 6.8$ Hz, H-16), 1.18 (q, $J = 6.8$ Hz, H-17), 1.30–1.22 (m, H-18), 1.30–1.22 (m, H-19), 1.30–1.22 (m, H-20), 1.30–1.22 (m, H-21), 1.33 (sextet, $J = 6.8$ Hz, H-22), 0.92 ppm (t, $J = 6.8$ Hz, H-23); ^{13}C NMR: $\delta = 150.1$ (C-1,8), 135.7 (C-2,7), 131.2 (C-3,6), 124.0 (C-4,5), 167.3 (C-9), 34.3 (C-10), 23.2 (C-11), 27.4 (C-12), 28.6 (C-13), 28.9 (C-14), 29.4 (C-15), 29.6 (C-16), 29.5 (C-17), 29.7 (C-18), 29.7 (C-19), 29.8 (C-20), 32.8 (C-21), 22.8 (C-22), 14.2 ppm (C-23); ^{29}Si NMR: $\delta = -222.6$ ppm; elemental analyses calcd (%) for $C_{62}H_{74}N_8O_4Si$: C 72.77, H 7.29, N 10.95; found: C 72.94, H 7.51, N 11.11. Suitable crystals for the X-ray diffraction study were obtained in a 3:2 solution of hexanes and dichloromethane.

Compound PcSi[$O_2C(CH_2)_{20}CH_3$]$_2$ (3f): Blue powder, yield 63%, m.p. = 120–122 °C. IR (KBr pellets): $\tilde{\nu} = 2957$, 2924, 2853, 1682, 1611, 1527, 1467, 1431, 1378, 1337, 1285, 1264, 1165, 1123, 1081, 913, 760, 739, 721 cm^{-1}; UV ($CHCl_3$): $\lambda = 290$, 322, 365, 372, 620, 653, 667, 695 nm; ^{1}H NMR: $\delta = 8.38$ (dd, $J_o = 5.5$, $J_m = 2.9$ Hz, H-3,6), 9.70 (dd, $J_o = 5.5$, $J_m = 2.9$ Hz, H-4,5), −0.64 (t, $J = 7.3$ Hz, H-10), −0.95 (q, $J = 7.3$ Hz, H-11), −0.74 (q, $J = 7.3$ Hz, H-12), 0.08 (q, $J = 7.3$ Hz, H-13), 0.54 (q, $J = 7.3$ Hz, H-14), 0.83 (q, $J = 7.3$ Hz, H-15), 1.06 (q, $J = 7.3$ Hz, H-16), 1.18 (q, $J = 7.3$ Hz, H-17), 1.34–1.19 (m, H-18), 1.34–1.19 (m, H-19), 1.34–1.19 (m, H-20), 1.34–1.19 (m, H-21), 1.34–1.19 (m, H-22), 1.34–1.119 (m, H-23), 1.34–1.19 (m, H-24), 1.34–1.19 (m, H-25), 1.34–1.19 (m, H-26), 1.34–1.19 (m, H-27), 1.34–1.19 (m, H-28), 1.34–1.19 (m, H-29), 0.90 ppm (t, $J = 7.3$ Hz, H-30); ^{13}C NMR: $\delta = 150.0$ (C-1,8), 135.7 (C-2,7), 131.2 (C-3,6), 124.0 (C-4,5), 167.3 (C-9), 34.3 (C-10), 23.2 (C-11), 27.4 (C-12), 28.6 (C-13), 28.9 (C-14), 29.4 (C-15), 29.6 (C-16), 29.8 (C-17), 29.8 (C-18), 29.8 (C-19), 29.8 (C-20), 29.8 (C-21), 29.8 (C-22), 29.8 (C-23), 29.8 (C-24), 29.8 (C-25), 29.8 (C-26), 29.8 (C-27), 32.8 (C-28), 22.7 (C-29), 14.1 ppm (C-30); ^{29}Si NMR: $\delta = -222.7$ ppm; elemental analyses calcd (%) for $C_{76}H_{102}N_8O_4Si$: C 74.84, H 8.43, N 9.19; found: C 75.02, H 8.52, N 9.31. Suitable crystals for the X-ray diffraction study were obtained in a 6:1 solution of hexanes and dichloromethane.

X-ray crystallography: X-ray diffraction analyses were carried out with an Enraf-Nonius FR590 Kappa-CCD diffractometer with $Mo_{K\alpha}$ radiation ($\lambda = 0.71073$ Å, graphite monochromator, $T = 293$ K, CCD rotation images). The crystals were glued to glass fibre sticks. Absorption correction was not necessary for compound **3a** as a result of systematic scaling integration of the reflections; for **3b** and **3c** empirical corrections were made to the data set using MULTISCAN.[31] The data for all structures were corrected for Lorentz and polarisation effects. The X-ray structures were solved by SHELXS-97 and SHELXL-97[32] was used for the refinement and data output; both programs were run using the WIN-GX[33] package. The structural images were prepared with ORTEP 3[34] and Mercury 1.2[35] programs. All non-hydrogen atoms were found by Fourier map differences and were fully refined by using anisotropic thermal parameters. Only some of the hydrogen atoms were determined by using difference Fourier maps and refined with one overall isotropic thermal parameter, the remaining hydrogen atoms were calculated geometrically. CCDC-264222 (**3a**), CCDC-264223 (**3c**), CCDC-264224 (**3d**), CCDC-264225 (**3e**) and CCDC-264226 (**3f**) contain the supplementary crystallographic data for this paper. These data can be obtained free of charge from The Cambridge Crystallographic Data Centre via www.ccdc.cam.ac.uk/data_request/cif.

Acknowledgements

The present study was partially supported by the Programa de Ingeniería Molecular-IMP (project number D.00161). We are grateful to Prof. R. Santillan for his helpful comments as well as for the kind revision of the manuscript.

[1] F. H. Moser, A. L. Thomas, *Phthalocyanine Compounds*, Reinhold Publishing Corp, New York, **1963**, p. 2.
[2] H. Engelkamp, S. Middelbeek, R. M. J. Nolte, *Science* **1999**, *284*, 785–788.
[3] J. L. Brédas, C. Adant, C. Tackx, A. Persoons, *Chem. Rev.* **1994**, *94*, 243–278.
[4] N. Kobayashi, *Coord. Chem. Rev.* **2002**, *227*, 129–152.
[5] H. B. Wang, L. S. Wang, *Nature* **1999**, *400*, 245–248.
[6] B. Crone, A. Bodabalapur, Y. Y. Lin, R. W. Filas, Z. Bao, L. A. LaDuca, R. Sarpeshkar, H. E. Katz, W. Li, *Nature* **2000**, *403*, 521–523.
[7] D. Voss, *Nature* **2000**, *407*, 442–444.
[8] Q. M. Zhang, H. Li, M. Poh, X. Feng, Z. Y. Cheng, H. Xu, C. Huang, *Nature* **2002**, *419*, 284–287.
[9] M. A. Baldo, D. F. O'Brien, Y. You, A. Shoustikov, S. Sibley, M. E. Thompson, S. R. Forrest, *Nature* **1998**, *395*, 151–154.
[10] N. Kobayashi, *Coord. Chem. Rev.* **2001**, *219–221*, 99–123.
[11] C. C. Leznoff, A. B. P. Lever, *Phthalocyanines: Properties and Applications*, **1989–1996**, *Vols. 1–4*, Wiley, New York.
[12] M. K. Engel, *Kawamura Rikagaku Kenkyusho Hokoku* **1997**, *8*, 11–54.
[13] The United Kingdom Chemical Database Service: D. A. Fletcher, R. F. McMeeking, D. Parkin, *J. Chem. Inf. Comput. Sci.* **1996**, *36*, 746–747.
[14] a) F. H. Allen, O. Kennard, *Chem. Des. Automation News* **1993**, *8*, 1; b) 3D Search and Research using the Cambridge Structural Database: F. H. Allen, O. Kennard, *Chem. Des. Automation News* **1993**, *8*, 31–37.
[15] a) M. Brewis, G. J. Clarkson, M. Helliwell, A. M. Holder, N. B. McKeown, *Chem. Eur. J.* **2000**, *6*, 4630–4636; b) N. B. McKeown, *J. Mater. Chem.* **2000**, *10*, 1979–1995; c) M. Brewis, M. Hewlliwell, N. B. McKeown, *Tetrahedron* **2003**, *59*, 3863–3872.
[16] a) M. Kimura, Y. Sugihara, T. Muto, K. Hanabusa, H. Shirai, N. Kobayashi, *Chem. Eur. J.* **1999**, *5*, 3495–3500; b) T. Uchiyama, K. Ishii,

T. Nonomura, N. Kobayashi, S. Isoda, *Chem. Eur. J.* **2003**, *9*, 5757–5761; c) N. Kobayashi, A. B. P. Lever, *J. Am. Chem. Soc.* **1987**, *109*, 7433–7441.

[17] a) B. Görlach, M. Dachtler, T. Glaser, K. Albert, M. Hanack, *Chem. Eur. J.* **2001**, *7*, 2459–2465; b) S. Knecht, K. Dürr, G. Schmidt, L. R. Subramanian, M. Hanack, *J. Porphyrins Phthalocyanines* **1999**, *3*, 292–298.

[18] a) J. Silver, C. S. Frampton, G. R. Fern, D. A. Davies, J. R. Miller, J. L. Sosa-Sanchez, *Inorg. Chem.* **2001**, *40*, 5434–5439; b) J. Silver, J. L. Sosa-Sanchez, C. S. Frampton, *Inorg. Chem.* **1998**, *37*, 411–417.

[19] a) N. Kobayashi, H. Miwa, V. N. Nemykin, *J. Am. Chem. Soc.* **2002**, *124*, 8007–8020; b) N. Kobayashi, T. Fukuda, K. Ueno, H. Ogino, *J. Am. Chem. Soc.* **2001**, *123*, 10740–10741.

[20] a) H. I. Beltran, R. Esquivel, A. Sosa-Sánchez, J. L. Sosa-Sánchez, H. Höpfl, V. Barba, N. Farfán, M. Galicia-García, O. Olivares-Xometl, L. S. Zamudio-Rivera, *Inorg. Chem.* **2004**, *43*, 3555–3556; b) H. I. Beltrán, R. Esquivel, M. Lozada-Cassou, M. A. Dominguez-Aguilar, A. Sosa-Sánchez, J. L. Sosa-Sánchez, H. Höpfl, V. Barba, R. Luna-García, N. Farfán, L. S. Zamudio-Rivera, *Chem. Eur. J.* **2005**, in press.

[21] a) E. A. Williams, *Ann. Clin. Res. Suppl. Ann. Rep. NMR Spectros.* **1983**, *15*, 235–289; b) E. Gómez, V. Santes, V. de la Luz, N. Farfán, *J. Organomet. Chem.* **1999**, *590*, 237–241; c) E. Gómez, V. Santes, V. de la Luz, N. Farfán, *J. Organomet. Chem.* **2001**, *622*, 54–60; d) E. Gómez, Z. Hernández, C. Álvarez-Toledano, R. A. Toscazo, V. Santes, P. Sharma, *J. Organomet. Chem.* **2002**, *648*, 280–287.

[22] a) J. A. Cella, J. D. Cargioli, E. A. Williams, *J. Organomet. Chem.* **1980**, *186*, 13–17; b) H. C. Marsmann, R. Löwer, *Chem. Z.* **1973**, *97*, 660–664.

[23] T. Koyama, T. Suzuki, K. Hanabusa, H. Shirai, N. Kobayashi, *Inorg. Chim. Acta* **1994**, *218*, 41–45.

[24] J. R. Mooney, C. K. Choy, K. Knox, M. E. Kenney, *J. Am. Chem. Soc.* **1975**, *97*, 3033–3038.

[25] D. A. Davies, C. Schnik, J. Silver, J. L. Sosa-Sanchez, P. G. Riby, *J. Porphyrins Phthalocyanines* **2001**, *5*, 376–380.

[26] *The Aldrich library of ^{13}C and ^{1}H FT-NMR spectra*, Aldrich Chemical Co., 1st ed., **1992**.

[27] C. Farren, S. FitzGerald, M. R. Bryce, A. Beeby, A. S. Batsanov, *J. Chem. Soc., Perkin Trans. 2* **2002**, 59–66.

[28] A. R. Kane, R. G. Yalman, M. E. Kenney, *Inorg. Chem.* **1968**, *7*, 2588–2592.

[29] A. R. Kane, J. F. Sullivan, D. H. Kenney, M. E. Kenney, *Inorg. Chem.* **1970**, *9*, 1445–1448.

[30] T. Fukuda, E. A. Makarova, E. A. Luk′yanets, N. Kobayashi, *Chem. Eur. J.* **2004**, *10*, 117–133.

[31] PLATON: A. L. Spek, *Acta Crystallogr. Sect. A* **1990**, *46*, C-34.

[32] SHELX-97, Program for Crystal Structure Solution, G. M. Sheldrick, University of Göttingen (Germany), **1993**.

[33] Win-GX program set: L. J. Farrugia, *J. Appl. Crystallogr.* **1999**, *32*, 837–838.

[34] ORTEP 3 program: L. J. Farrugia, *J. Appl. Crystallogr.* **1997**, *30*, 565–566.

[35] Mercury 1.2.1, Copyright CCDC **2001–2004**, all rights reserved. For more information about this application, please contact User Support by e-mail at: support@ccdc.cam.ac.uk, or at the www site http://www.ccdc.cam.ac.uk/mercury/.

Received: January 3, 2005
Published online: May 2, 2005

